hydrogen bonds between C-3 OH and the carboxyl. It seems difficult to invoke an intermolecular hydrogen bond without having some sort of added hydrophobic contribution in aqueous solution. This kind of effect has been observed in aliphatic carboxylic acids—larger aliphatic chains leading to stronger dimerization effects in aqueous solution.[32] To describe the ^{13}C NMR shifts as due to intermolecular hydrogen bonding seems too simple for aqueous solutions of NaDC. Perhaps some partial hydrophobic interactions, which may be back-to-back hydrophobic interaction between bile salt molecules, occur in the initial aggregation, and this then changes when the "normal" micelles begin to form. Desnoyers[33] suggested that the model of the partial hydrophobic interaction in the polymer-like aggregate may be Fujiyama's model; i.e., water molecules lie between hydrophobic molecules.[34] The decrease of the partial molal volume with the concentration in the lower concentration range (see Figure 2) can probably be interpreted by the model. Further investigation is needed to decide whether the partial hydrophobic interaction in the polymer-like aggregate is of Fujiyama's model or not.

It may be concluded that, as has been suggested from various experiments, the intermolecular hydrogen bonding between the OH group at the 3 position and the COOH group and partial hydrophobic interaction (back-to-back) contribute to the formation of polymer-like (ordered) aggregates in the lower concentration range and that, with increasing NaDC concentration, the polymer-like aggregates change into smaller aggregates accompanying the breakdown of hydrogen bonding and the enhancement of hydrophobic bonding, as is indicated by the upfield shift of methyl-group carbons and by the abrupt increase in the partial molal volume.

Acknowledgment. We thank Professor J. P. Kratohvil, Professor J. E. Desnoyers, and the reviewers of this paper for a great deal of advice. We are indebted to our coworkers for experimental assistance. The present work has been performed within a research program sponsored by Central Research Institute of Fukuoka University.

(32) P. Mukerjee, K. J. Mysels, and C. I. Dulin, *J. Phys. Chem.*, **62**, 1390 (1958).
(33) J. E. Desnoyers, private communication at the 6th International Symposium on Solute–Solute–Solvent Interaction, Minoo Osaka, Japan, 1982.
(34) N. Ito, T. Kato, and T. Fujiyama, *Bull. Chem. Soc. Jpn.*, **54**, 2573 (1981).

Viscosity Dependence of the Rotational Reorientation of Rhodamine B in Mono- and Polyalcohols. Picosecond Transient Grating Experiments

R. S. Moog, M. D. Ediger, S. G. Boxer, and M. D. Fayer*

Department of Chemistry, Stanford University, Stanford, California 94305 *(Received: May 24, 1982; In Final Form: August 17, 1982)*

Rotational reorientation times (τ_{ROT}) were obtained for rhodamine B in a series of *n*-alcohols and polyalcohols of varying viscosities by a transient grating technique. The general trend of the Debye–Stokes–Einstein (DSE) theory was shown to extend to much higher viscosities than previously reported. Detailed analysis of the results suggests that the *n*-alcohols and polyalcohols provide two distinct hydrodynamic boundary conditions for the rotating species. In the *n*-alcohols, stick boundary conditions are observed, while the polyalcohols provide approximately slip boundary conditions. The question of a difference in the rotation times for the ground and excited electronic states is addressed and an upper bound is placed on this difference for rhodamine B.

Introduction

The study of rotational reorientation of molecules in liquid solvents has been used as a probe of solute conformations,[1] solvent–solute interactions,[2-6] and local solvent structure.[7] An understanding of molecular orientation and rotation in liquids is also important in the context of chemical reaction dynamics.[8] Over 10 years ago, the first direct observation of rotational reorientation of molecules in a liquid solvent using picosecond laser pulses was reported.[9] Since then several other workers have applied picosecond spectroscopic techniques to the study of rotational motion.[5,10-14] Various dye molecules in a series of solvents of different viscosities have been examined, and the results have been compared to the predictions of De-

(1) Fleming, G. R.; Knight, A. E. W.; Morris, J. M.; Robbins, R. J.; Robinson, G. W. *Chem. Phys. Lett.* **1977**, *49*, 1.
(2) Scholz, M.; Teuchner, K.; Nather, M.; Becker, W.; Dahne, S. *Acta Phys. Pol. A* **1978**, *54*, 823.
(3) Klein, U. K. A.; Haar, H. P. *Chem. Phys. Lett.* **1978**, *58*, 531.
(4) Millar, D. P.; Shah, R.; Zewail, A. H. *Chem. Phys. Lett.* **1979**, *66*, 435.
(5) von Jena, A.; Lessing, H. E. *Chem. Phys.* **1979**, *40*, 245; *Chem. Phys. Lett.* **1981**, *78*, 187.
(6) Shapiro, S. L.; Winn, K. R. *Chem. Phys. Lett.* **1980**, *71*, 440.
(7) Beddard, G. S.; Doust, T.; Hudales, J. *Nature (London)* **1981**, *294*, 145.
(8) Steiger, U. R.; Keizer, J. *J. Chem. Phys.* **1982**, *77*, 777.
(9) Eisenthal, K. B.; Drexhage, K. H. *J. Chem. Phys.* **1969**, *51*, 5720.
(10) Phillion, Donald W.; Kuizenga, Dirk J.; Siegman, A. E. *Appl. Phys. Lett.* **1975**, *27*, 85.
(11) Fleming, G. R.; Morris, J. M.; Robinson, G. W. *Chem. Phys.* **1976**, *17*, 91.
(12) Eichler, H. J.; Klein, U.; Langhans, D. *Chem. Phys. Lett.* **1979**, *67*, 21.
(13) Beddard, Godfrey, S.; Doust, Tom; Porter, George *Chem. Phys.* **1981**, *61*, 17.
(14) van Resandt, R. W. W.; de Maeyer, L. *Chem. Phys. Lett.* **1981**, *78*, 219. Spears, K. G.; Cramer, L. E. *Chem. Phys.* **1978**, *30*, 1.

0022-3654/82/2086-4694$01.25/0

bye–Stokes–Einstein (DSE) hydrodynamic theory.[15] This theory considers a sphere of radius R and hydrodynamic volume V rotating in a fluid continuum of macroscopic viscosity η and relates the rotational reorientation time, τ_{ROT}, to the viscosity according to the equation

$$\tau_{ROT} = \frac{8\pi\eta R^3}{6kT} = \frac{\eta V}{kT} \quad (1)$$

This relation is derived by using hydrodynamic theory with stick boundary conditions. In this formalism the fluid at the surface of the model solute rotates along with the solute. Although the applicability of this relation to the rotation of large aspherical molecules in discrete solvents is not obvious, a general consensus from these studies has been that cationic dye molecules (M_r 300–1000) in hydrogen-bonding solvents (usually n-alcohols) of viscosity less than 15 cP do tend to follow the prediction of the stick hydrodynamic theory. For particular dyes, both positive[16] and negative[17] experimental deviations from DSE theory have been reported for the larger members of the n-alcohol homologous series. Nevertheless, the general trend predicted by hydrodynamic theory is observed.

Anomalously short rotation times have been observed for dye molecules in ethylene glycol relative to 1-decanol.[5] Although ethylene glycol is significantly more viscous than 1-decanol, rhodamine molecules have been consistently reported to rotate 5-10% faster in glycol.[5,16] Previous workers suggested that this implies that the rotating molecule "does not view the full frictional effects of the polymeric structure of the solvent" (ethylene glycol).[16] Others propose that there are "special interactions" with the solvent that are observed in either type of alcohol, but that "the absolute τ_{ROT} values contain a microfriction contribution that is rather weakly correlated with η."[5]

In the present study, the rotational motion of rhodamine B is examined in a series of n-alcohols and in mixtures of ethylene glycol and glycerol of varying viscosities.[18] Our results demonstrate that the linear correlation between τ_{ROT} and η is approximately valid through a much higher viscosity regime than previously reported[19] but that the hydrodynamic boundary condition is different for n-alcohols (stick) and glycol–glycerol mixtures (slip). A simple qualitative model is proposed to account for this difference. This model suggests that the relatively fast rotation of rhodamine B in ethylene glycol (and other polyalcohols) arises from differences in the solvent structure rather than differences in solvent–solute interactions.

Many smaller molecules have been observed to rotate according to hydrodynamic theory, but with a slip boundary condition.[20] In this model there is no tangential component of stress on the rotating body. Therefore, a spherical rotator would have a viscosity-independent τ_{ROT} under these conditions. For bodies of other shapes, the slip boundary condition results in rotational reorientation times which are a linear function of solvent viscosity. Thus, in general, stick and slip boundary conditions both produce a linear viscosity dependence.

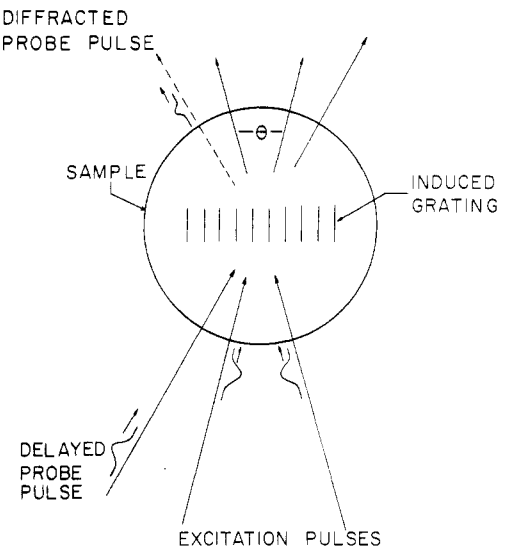

Figure 1. Schematic illustration of the transient grating experiment. Interference between the incoming excitation pulses results in a spatially periodic density of excited states, which Bragg diffracts the subsequent probe pulse. The diffracted probe is the signal. In the actual experiment, the probe pulse and, therefore, the diffracted signal are nearly collinear with the excitation beams. The separation has been exaggerated for clarity.

Experimental systems are commonly modeled as oblate or prolate ellipsoids. Although solute rotation is generally described for such cases by two rotational reorientation times, experimental measurements of the type described here are usually fitted with single reorientation times.[11,21] This is physically reasonable for rhodamine B and similar solutes. Then, V in the DSE relation can be replaced by V_{eff}, the effective spherical volume of the rotating body.

A modified DSE equation can now be written which includes the two limiting hydrodynamic boundary conditions:

$$\tau_{ROT} = fV_{eff}\eta/kT \quad (2)$$

where $f = 1$ for stick boundary conditions and $f = f(\rho)$ for slip boundary conditions, where ρ is the axial ratio. The values of $f(\rho)$ have been tabulated for oblate and prolate ellipsoids.[22]

Experimental Section

Picosecond transient grating experiments are well-known in a variety of contexts and have been described in detail previously.[23,24] In this work, two picosecond excitation pulses (less than 50-ps fwhm) having parallel polarization were crossed spatially and temporally in the sample under investigation. The crossed excitation pulses produce an optical interference pattern (see Figure 1). Optical absorption produces a spatially periodic distribution of excited states which mimics the interference pattern. A corresponding periodic spatial variation in the index of refraction results.[25] The diffraction efficiency of this induced diffraction grating decays in time due to several processes. A delayed probe pulse, with a known polarization relative to that which created the grating, is diffracted off the grating at some later time.

A detailed analysis of the time dependence of this diffracted signal due to molecular rotations has been pres-

(15) Einstein, A. *Ann. Phys. (Leipzig)* **1906**, *19*, 371; English translation in: "Investigations on the Theory of the Brownian Movement"; Dover: New York, 1956.
(16) Chuang, T. J.; Eisenthal, K. B. *Chem. Phys. Lett.* **1971**, *11*, 368.
(17) Porter, G.; Sadkowski, P. J.; Tredwell, C. J. *Chem. Phys. Lett.* **1977**, *49*, 416.
(18) Previously reported data (see ref 19) in the high-viscosity regime appear to contain serious systematic errors due to improper tail-matching normalization of the data and possible fluorescence reabsorption.
(19) Rice, Stephan A.; Kenney-Wallace, G. A. *Chem. Phys.* **1980**, *47*, 161.
(20) Bauer, D. R.; Brauman, J. I.; Pecora, R. *J. Am. Chem. Soc.* **1974**, *96*, 6840.
(21) Tau, Terence *Biopolymers* **1969**, *8*, 609.
(22) Hu, Chih-Ming; Zwanzig, Robert *J. Chem. Phys.* **1974**, *60*, 4354.
(23) Eichler, H. J. *Opt. Acta* **1977**, *24*, 631. Fayer, M. D. *Annu. Rev. Phys. Chem.* **1982**, *33*, 63.
(24) von Jena, A.; Lessing, H. E. *Opt. Quantum Electron.* **1979**, *11*, 419.
(25) Nelson, K. A.; Casalegno, Roger; Miller, R. J. Dwayne; Fayer, M. D. *J. Chem. Phys.*, **1982**, *77*, 1144.

ented by von Jena and Lessing.[24] We follow their analysis but assume negligible triplet production, justified for our system by the observed experimental decays (see Figures 3 and 4). Time-dependent signals, $T_{\parallel}(t)$ and $T_{\perp}(t)$, are obtained when the probe pulse polarization is oriented parallel or perpendicular to the polarization of the excitation pulses.

$$T_{\parallel}(t) = K\{[1 + 2C \exp(-t/\tau_{ROT})] \exp(-t/\tau_F)\}^2 \quad (3)$$

$$T_{\perp}(t) = K\{[1 - C \exp(-t/\tau_{ROT})] \exp(-t/\tau_F)\}^2 \quad (4)$$

τ_{ROT} and τ_F are the rotational reorientation time and the fluorescence lifetime, respectively, and K is a proportionality constant which is a function of a variety of time-independent parameters. C is a constant whose value depends on the degree of photoselection; in an ideal system, $C = 0.4$. In practice C is less than 0.4 and can be obtained experimentally from the $t = 0$ data. However, the value of C does not enter into our data analysis. If the polarization of the probe is set at 54.7° from the excitation polarization (the "magic angle"), the observed decay is independent of rotational dynamics. This decay is described by

$$T_M(t) = K \exp(-2t/\tau_F) \quad (5)$$

Thus, this signal decays as a single exponential with a lifetime exactly half the fluorescence lifetime. The fluorescence lifetime of the solute molecules can also be obtained by forming the sum

$$S(t) = [T_{\parallel}(t)]^{1/2} + 2[T_{\perp}(t)]^{1/2} = 3K^{1/2} \exp(-t/\tau_F) \quad (6)$$

The rotational reorientation time can be determined by computing the difference

$$D(t) = [T_{\parallel}(t)]^{1/2} - [T_{\perp}(t)]^{1/2}$$

$$= 3K^{1/2}C \exp(-t/\tau_{ROT}) \exp(-t/\tau_F) \quad (7)$$

Then

$$R(t) \equiv D(t)/S(t) = C \exp(-t/\tau_{ROT}) \quad (8)$$

When the experimentally obtained decays are combined in this manner, a single exponential function is produced whose decay time is equal to the rotational reorientation time.

Transient grating experiments were performed with the apparatus illustrated in Figure 2. The 1.06-μm output of a continuously pumped acoustooptically Q-switched and mode-locked Nd:YAG laser was frequency doubled, and the 532-nm component, a train of about 40 pulses, was used to synchronously pump a rhodamine 6G dye laser at 400 Hz. The dye laser was cavity dumped, resulting in a single pulse at 556 nm of about 4 μJ. This output was split into two components of about 70% and 30% intensity. The weaker component was the probe pulse and was passed down a motorized continuous delay line to provide the time variation in the experiment. The stronger component of the optical pulse was split again to provide the two equally intense excitation beams which created the transient grating. A half-wave plate was placed in the probe beam path to permit variation of the probe pulse polarization relative to that of the excitation pulses. This allowed acquisition of each of the time-resolved signals $T_{\parallel}(t)$, $T_{\perp}(t)$, and $T_M(t)$. The pulse intensities were attenuated until further attenuation produced no perceptible change on the decay curves.[26]

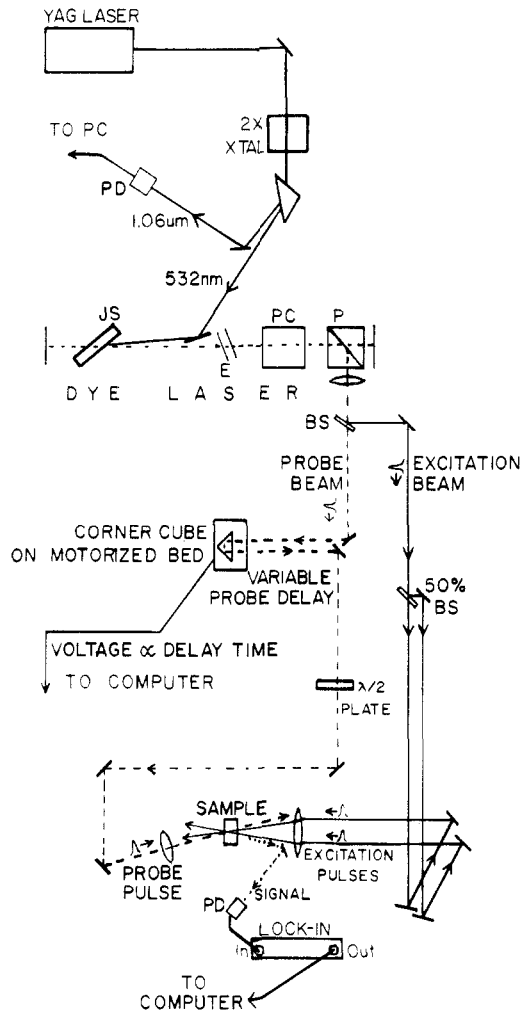

Figure 2. Transient grating experimental setup: PC = Pockels cell; P = polarizer; PD = photodiode; JS = jet stream; E = etalon; BS = beam splitter.

One of the excitation beams was chopped at half the laser pulse rate, and the diffracted signal was spatially isolated and then monitored by a photodiode and lock-in amplifier. Since the laser was run at a high repetition rate and the delay line was run slowly, many laser shots were averaged to produce a grating signal for any delay line position.

Each sweep of the delay line took about 15 min and was stored separately by a computer. The power variation of the laser output over this time was less than ±2%. Several sweeps for each of the three polarizations were recorded for each solvent studied to check reproducibility. They were then averaged to improve the signal-to-noise ratio.

All samples were dilute solutions of rhodamine B. A very small amount of concentrated HCl was added[27] to eliminate any possible ambiguities caused by the acid–base equilibrium at the carboxyl group.[28] The sample holder was a rotating cell of approximately 5.0-cm diameter formed by two optical flats separated by thin (180 μm) spacers. All of the samples had absorption maxima between 550 and 565 nm, and the maximum optical density was always between 0.025 and 0.040.[26]

The viscosity measurements were made with Ostwald viscosimeters using standard techniques.[29] All measure-

(26) Under these conditions, the errors from reabsorption and stimulated emission are negligible. Hammond, P. R. *J. Chem. Phys.* **1979**, *70*, 3884.

(27) The volume of solution added was less than 0.5% of the total solvent volume.

(28) Sadkowski, P. J.; Fleming, G. R. *Chem. Phys. Lett.* **1978**, *57*, 526.

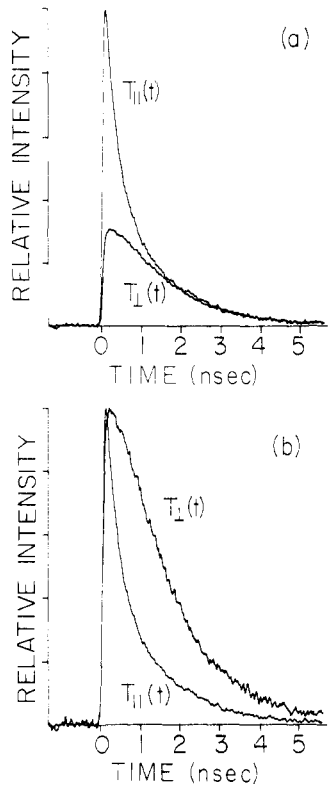

Figure 3. Time decays of the transient grating signal with probe pulse polarization parallel to ($T_{\parallel}(t)$) and perpendicular to ($T_{\perp}(t)$) the excitation polarization for a sample of rhodamine B in 1-propanol. (a) Correct relative intensities of the two curves showing merging of the curves at times for which significant signal can be observed. This is indicative of fast rotation. (b) The same data adjusted to have identical maxima. Note that the two curves have vastly different shapes.

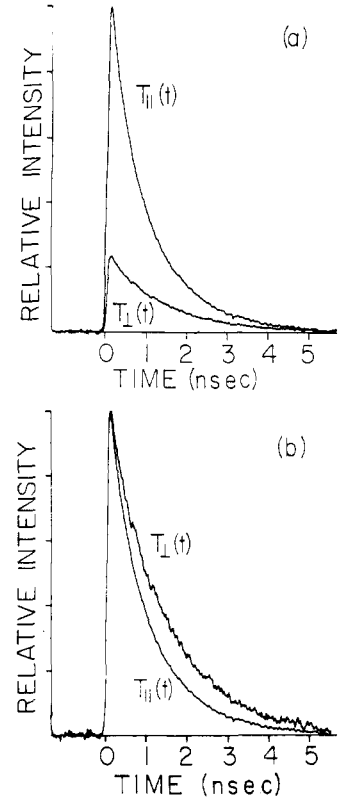

Figure 4. Time decays $T_{\parallel}(t)$ and $T_{\perp}(t)$ for a sample of rhodamine B in 1-decanol. (a) Correct relative intensities of the two curves showing merging of the curves only when the signal has fallen to approximately zero. (b) The same data ajusted to have identical maxima. Note that the two curves have shapes more similar than in Figure 3b.

ments were made on aliquots of solvent which were identical with those used in the time-dependent experiments. The viscosity determination was done during the appropriate transient grating experiment to ensure that the measured viscosity was the true sample viscosity. The room temperature was constant to within ±0.3 °C during the runs for a particular solvent. Several runs were made for each solvent, and the average calculated viscosity was used.

Results

Figure 3 shows results for decay sweeps $T_{\parallel}(t)$ and $T_{\perp}(t)$ in 1-propanol, a solvent in which the rotation time is short compared to the singlet excited-state lifetime. Note that at long times the two curves coalesce in Figure 3a, as would be expected after rotational diffusion has randomized the initial anisotropic distribution of ground and excited states. Figure 3b reproduces these two curves after they are adjusted to have identical intensities at their maxima. The short rotation time causes the two curves to have vastly different shapes. In Figure 4, the equivalent data for 1-decanol are shown. In this solvent the rotation time and the excited-state lifetime are approximately equal. As seen in Figure 4a, the two curves do not meet until the signal is nearly gone. Figure 4b shows that the shapes of $T_{\parallel}(t)$ and $T_{\perp}(t)$, while still distinguishable because of molecular rotation, are not nearly as different as in the propanol case. The two curves obtained with glycerol as the solvent were virtually indistinguishable in shape, although their magnitudes were quite different. Gochanour and Fayer[30] reported a similar observation for rhodamine 6G in glycerol using a fluorescence mixing technique. Thus, dye molecule rotation in glycerol must occur on a time scale which is *very long* compared to the fluorescence lifetime.[18] Therefore,

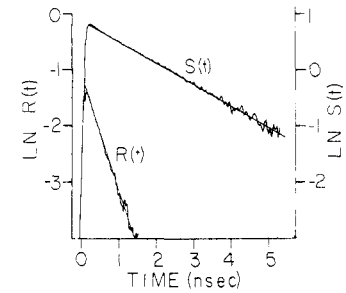

Figure 5. $S(t)$ and $R(t)$ curves calculated from the data presented in Figure 3. The straight-line fits yield values of the fluorescence lifetime (τ_F) and the rotational reorientation time (τ_{ROT}), respectively, for rhodamine B in 1-propanol. Values are listed in Table I.

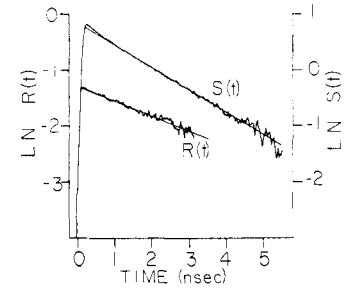

Figure 6. $S(t)$ and $R(t)$ curves calculated from the data presented in Figure 4. The straight-line fits yield values for τ_F and τ_{ROT}, respectively, for rhodamine B in 1-decanol. Values are listed in Table I.

(29) Shoemaker, D. P.; Garland, C. W.; Steinfeld, J. I. "Experiments in Physical Chemistry"; McGraw-Hill: New York, 1974.
(30) Gochanour, C. R.; Fayer, M. D. *J. Phys. Chem.* 1981, *85*, 1989.

TABLE I

solvent	η,[b] cP	τ_F,[c] ns	τ_F,[d] ns	τ_{ROT},[e] ps
ethanol[a]	1.2			260 (+20, −20)
ethanol	1.31	2.16	2.23	265 (+10, −10)
propanol[a]	2.23			460 (+30, −30)
propanol	2.51	2.60	2.62	480 (+15, −15)
heptanol	7.42	2.32	2.62	1850 (+150, −350)
decanol[a]	13.5			3050 (+250, −250)
decanol	16.7	2.44	2.41	3800 (+250, −250)
ethylene glycol[a]	19.5			2800 (+200, −200)
ethylene glycol	24.2	2.56	2.61	3700 (+250, −250)
mixture 1	33.4	2.57	2.82	5600 (+300, −300)
mixture 2	43.1	2.75	2.86	6600 (+500, −900)
mixture 3	80.1	2.91	2.96	13500 (+3000, −2000)
mixture 4	356	3.05	3.08	26000 (+9000, −4000)
glycerol	1770	3.18	3.25	>57000

[a] Data from ref 5. Viscosities are lower than in the present work because the temperature was higher (293 K). [b] All values of η are ±1%. [c] Obtained from $T_M(t)$. All values of τ_F are ±50 ps. [d] Obtained from $S(t)$. All values of τ_F are ±50 ps. [e] Obtained from $R(t)$ in the present work. Errors in the reported values are listed in parentheses. Note that in some cases the error range is not symmetric.

we report only a lower bound on the rotation time in glycerol.

One of the difficulties associated with previous experiments is the proper normalization of the two separate decays.[31] Tail-matching[11-13,17,19,34] and leading-edge-matching[11,13,19] techniques have been used to correct shot-to-shot pulse intensity variations. The long-term stability of the laser system used in our experiments provides curves which do not require subsequent normalization.[35] A check on the validity of the data handling is the fact that the sum $S(t)$ (eq 6) yields a purely exponential decay with a lifetime equal to the fluorescence lifetime obtained from $T_M(t)$. Figures 5 and 6 show the calculated $S(t)$ curves, obtained from the data in Figures 3 and 4. In Table I, the lifetimes obtained from these two methods are listed for all of the solvents studied and the agreement is generally very good. The reasons for the small discrepancies for heptanol and mixture 1 are not known.

$R(t)$ results for the same data sets are also shown in Figures 5 and 6. Although at long times the signal-to-noise ratio decreases significantly, a good fit to a single exponential decay is realized in all cases. The values obtained for τ_{ROT} are tabulated in Table I. Also reported in Table I are values of τ_{ROT} reported previously by von Jena and Lessing.[5] Their work was performed at a temperature different from ours; therefore, different viscosities, and correspondingly different rotation times, are obtained. All τ_{ROT} data listed in Table I are plotted in Figure 7.

Discussion

Hydrodynamic Boundary Conditions. Equation 2 can be rewritten

$$\log \tau_{ROT} = \log (\eta/T) + \log (fV_{eff}/k) \quad (9)$$

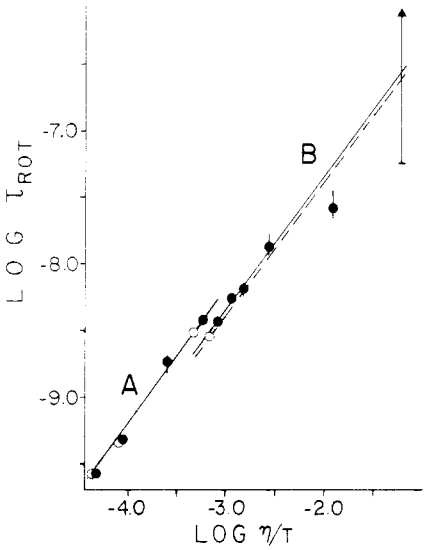

Figure 7. Plot of log τ_{ROT} (τ_{ROT} in seconds) vs. log η/T (η in poise and T is K) for rhodamine B. Filled circles are data from this work; open circles are previously reported data from ref 5. Error bars are shown for those data points which have uncertainties greater than the circle size. Details of each data point are given in Table I. The general predictions of the DSE theory are obeyed to high viscosity. The data are best fitted by two parallel lines of slope unit. Taking line A through the monoalcohol data to define the stick boundary condition, the dashed line represents the corresponding calculated slip boundary condition line. Line B through the polyalcohol data is very close to the slip line.

so that a plot of log τ_{ROT} vs. log η/T should have a slope of unity. Then, for a given boundary condition and molecular axial ratio, the y intercept yields a value for V_{eff} for the rotating body. As seen in Figure 7, the general correlation between τ_{ROT} and viscosity is obeyed over a wide viscosity range for the systems studied: as the viscosity is increased, the rotation times become slower. These results do not show a "saturation effect"[19] of viscosity in the ethylene glycol region (log $\eta/T \approx -3.1$).

The data are not fitted by a *single* line of unit slope. Rather, *two* parallel lines (lines A and B in Figure 7), each having unit slope but different y intercepts, provide better agreement with the data. Line A passes through the data obtained from n-alcohols, while line B passes through the polyalcohol data. In the most viscous solvents, the rotation times are more than 1 order of magnitude longer than the fluorescence lifetimes, making accurate values of τ_{ROT} difficult to obtain. Thus, no conclusions can be drawn about the applicability of the hydrodynamic theory at the highest viscosities.

The n-alcohols and polyalcohols are seen to comprise two distinct types of solvents. In each solvent type the relationship between solvent viscosity and τ_{ROT} obeys hydrodynamic prediction, but the value of fV_{eff} is different. In this context, the often noted decrease of τ_{ROT} from 1-decanol to ethylene glycol is not anomalous but is indicative of a change in the hydrodynamic boundary condition, the effective molecular volume, or both.

The difficulty of differentiating between the effects of changing boundary conditions and effective size has been mentioned by previous workers.[5,36] A difference in V_{eff} for the two solvent systems would imply a difference in solvent–solute interactions for the two different types of solvent. For the particular systems studied here, a reasonable argument can be made for explaining the results in terms of changing boundary conditions rather than differences in solvent–solute interactions.

(31) Recently, experimental techniques for obtaining $R(t)$ from a single decay curve have been developed. See ref 32 and 33.

(32) von Jena, A.; Lessing, H. E. *Ber. Bunsenges. Phys. Chem.* **1979**, *83*, 181.

(33) Waldeck, David H.; Fleming, Graham R. *J. Phys. Chem.* **1981**, *85*, 2614.

(34) Fleming, G. R.; Knight, A. E. W.; Morris, J. M.; Robbins, R. J.; Robinson, G. W. *Chem. Phys. Lett.* **1977**, *51*, 399.

(35) Other experimental techniques which provide decay curves which do not require normalization are presented in ref 4 and 14.

(36) Kenney-Wallace, Geraldine A. *Philos. Trans. R. Soc. London, Ser. A* **1980**, *299*, 309.

The most important solvent–solute interaction is hydrogen bonding. While hydrogen bonding to the solute can increase the value of V_{eff} relative to that observed for a noninteracting solute, this interaction would be expected to be much the same for the mono- and polyalcohols. Therefore, V_{eff} should be approximately constant for both series of solvents. In this case, the different intercepts obtained from Figure 7 are likely to correspond to different hydrodynamic conditions.

When one uses the data in Figure 7 and assumes stick boundary conditions, the calculated values for the effective volume of rhodamine B are V_{eff} = 900 Å^3 in the *n*-alcohols and V_{eff} = 640 Å^3 in the polyalcohols. A reasonable model for rhodamine B is an oblate ellipsoid with semiaxes of 2 and 7 Å for which V_{eff} is 750 Å^3.[11] Both experimentally obtained values are reasonably close to the model volume, considering the crudeness of the oblate ellipsoid approximation. Still, such a large change in V_{eff} for the two series of solvents seems unlikely, in light of the argument presented above. Therefore, we favor the notion that a change in boundary conditions is responsible for the two parallel lines in Figure 7.

The dashed line in Figure 7 corresponds to the slip boundary condition for an oblate ellipsoid with $\rho = {}^2/_7$, assuming that line A through the *n*-alcohol data corresponds to the stick boundary condition. This dashed line is very close to line B through the polyalcohol data, suggesting that the slip hydrodynamic boundary condition approximately applies in these solvents.

The difference between stick and slip boundary conditions is often related to the relative size of the solvent and solute molecules.[37] When the rotating solute molecule is larger than the surrounding solvent molecules, stick boundary conditions are expected to apply. In the case of solvent molecules which are large compared to the solute, slip hydrodynamics are expected. At first, this analysis appears inconsistent with our results. Ethylene glycol and glycerol are both much smaller than rhodamine B, but in these solvents approximately slip hydrodynamics are obeyed. However, these two polyalcohols are capable of forming large polymeric network-type structures, analogous to the interconnected quasi-lattice structure of water.[38] The effective "solvent" is then a species which extends over regions much larger than the size of rhodamine B. Thus, the polyalcohol solvent structure produces a slip boundary condition.

Since the *n*-alcohols are capable of forming dimers and also are expected to form small ring *n*-mers,[39] the applicability of the stick boundary condition in these solvents is not necessarily clear. This is especially true since the size of the alcohol molecule increases substantially from ethanol to decanol. The fact that *all* of our *n*-alcohol results fall on one line suggests that in this case the boundary condition is constant throughout the series.

The stick and slip boundary conditions define the extrema for the rotation of a body under hydrodynamic conditions. τ_{ROT} must lie between the values predicted by eq 2 for a particular viscosity and effective volume. A plot of eq 2 in the manner of Figure 7 for both hydrodynamic boundary conditions gives two parallel lines whose separation is determined by $f(\rho)$ for slip boundary conditions. This separation is dependent only on ρ given a fixed value of V_{eff}. For an oblate ellipsoid with $\rho = {}^2/_7$, this separation is shown in Figure 7 as the difference between line A and the dashed line. Note that the separation between line A and line B is almost as large as this maximal difference. Thus, if the boundary condition in *n*-alcohols were significantly different from stick, the values of τ_{ROT} for the polyalcohols would be smaller than the hydrodynamic minima predicted by slip boundary conditions. This analysis supports the proposition that the *n*-alcohol series approximately defines the stick boundary condition in this case.

In summary, the differences between the series of rotation times of rhodamine dyes in the *n*-alcohols and polyalcohols arise from differing hydrodynamic boundary conditions. The *n*-alcohols studied here define the stick boundary condition line. Assuming rhodamine B to be an oblate ellipsoid with $\rho = {}^2/_7$ and using the theoretical relationship between stick and slip boundary conditions, one obtains the dashed line in Figure 7. Within the error in modeling rhodamine B in this manner, Figure 7 shows that the series of polyalcohols approximately defines the slip boundary condition. The capacity to form widely extended hydrogen-bonded networks in these solvents allows the slip boundary condition to apply.

Ground- and Excited-State Rotation Times. The discussion thus far has assumed that the rotational reorientation time of the solute is identical in the ground and excited states. However, the difference in electronic structure in the two states could result in different interactions with the surrounding solvent molecules. Thus, the rotational dynamics of the ground-state molecule could be altered upon excitation. If τ_G and τ_E are the rotational reorientation times in the ground and excited states, respectively, and negligible triplet formation is assumed, then eq 6 can be rewritten in the more general form

$$D(t) = -3K^{1/2}C \exp(-t/\tau_G)\left[\frac{1 - \exp\{-t(1/\tau_D + 1/\tau_F)\}}{1 + \tau_F/\tau_D} - 1\right] \quad (10)$$

where $1/\tau_D = 1/\tau_E - 1/\tau_G$. Equation 8 becomes

$$R(t) = C \exp(-t/\tau_G)\left[\exp(t/\tau_F) - \frac{\exp(t/\tau_F) - \exp(-t/\tau_D)}{1 + \tau_F/\tau_D}\right] \quad (11)$$

Equations 10 and 11 were derived by assuming no excited-state absorption of the probe, a valid approximation for our experimental system. The derivation is analogous to that outlined previously by Eisenthal[40] for absorption dichroism studies, with suitable modifications included to allow for differences between the transient grating and absorption dichroism observables.

If $\tau_G = \tau_E$, then eq 11 reduces to eq 8 as expected. However, when $\tau_G \neq \tau_E$, the plot of $R(t)$ is not a single exponential decay but a complicated function of the rotation times and the excited-state lifetime. However, for many combinations of τ_F, τ_E, and τ_G, the resulting function approximates a single exponential very well over the time region in which the transient grating signal is observable. To determine the sensitivity of the theoretical $R(t)$ curve to the different rotation times, we combined various values of τ_G and τ_E with the experimental value of τ_F to generate plots of $R(t)$ for a particular solvent system. These curves were compared to the experimental $R(t)$ curves. Given the noise inherent in the experimentally obtained decays, there

(37) Acrivos, A., private communication.
(38) Andersen, Hans C., private communication.
(39) Anderson, Bradley D.; Rytting, J. Howard; Lindenbaum, Siegfried; Higuchi, Takeru *J. Phys. Chem.* **1975**, *79*, 2340.
(40) Eisenthal, K. B. *Acc. Chem. Res.* **1975**, *8*, 118.

are many possible combinations of τ_G and τ_E which are consistent with the experimental results.

At early times, the shape of the $R(t)$ curve is determined mainly by the ground-state rotation times, whereas at longer times the effects of the excited-state rotation time becomes more important. The signal-to-noise ratio is greatest at early times, so the acceptable values of τ_G extend over a relatively narrow range. The variations in τ_G are essentially the same as the uncertainties in τ_{ROT} listed in Table I. At longer times the noise increases, allowing a wider range in the values of τ_E which would be consistent with the observed results. We found that τ_E could be as much as 30% greater or less than τ_G and still be compatible with our experimental results.

The rotational reorientation results presented here are essentially measures of the ground-state rotation time of rhodamine B. Hence, possible differences in ground- a nd excited-state rotation times do not affect the discussion presented above. However, the excited-state rotation times could vary by as much as 30% from the ground-state values. Since fluorescence depolarization experiments examine *only* excited-state rotation, a careful study of a particular solvent–solute system using that technique and the transient grating (or transient absorption[4]) technique would provide a measure of the differences in excited-state and ground-state rotation times.

Acknowledgment. We thank Professor A. Acrivos, Chemical Engineering Department, and Professors Hans C. Andersen, R. Pecora, and J. I. Brauman, Chemistry Department, Stanford University, for interesting conversations pretaining to this work. We also acknowledge the National Science Foundation, DMR 79-20380 and PCM 79-26677, and the Department of Energy, DE-FG02-80CS84006, for supporting this work. S.G.B. acknowledges the Alfred P. Sloan Foundation and the Camille and Henry Dreyfus Foundation. M.D.E. thanks the National Science Foundation for a Predoctoral Fellowship.

Correlation Function Theory for Kerr-Effect Relaxation of Axially Symmetric Polar Molecules

Robert H. Cole

Department of Chemistry, Brown University, Providence, Rhode Island 02912 *(Received: May 27, 1982; In Final Form: August 2, 1982)*

Nonlinear response theory is used to obtain correlation function expressions for time-dependent electric birefringence following removal, application, and reversal of an external field polarizing a system of axially symmetric dipolar molecules. The role of collisions is essential in determining the second-order effects of permanent dipole torques on the field on and field reversal which randomize momenta in times short compared to those for significant reorientations. As for the special case of diffusional reorientation, the field-off response is determined by $P_2(\cos\theta(t))$ correlations only, otherwise both these correlations associated with optical anisotropy and $P_1(\cos\theta(t))$ correlations from dipole torques contribute to the effects. The results thus provide a basis for experimental evaluation of both functions from Kerr-effect measurements.

Introduction

Electric birefringence has proved to be a useful probe of changing molecular orientations produced by time-dependent applied fields, notably for studies of polymers in solution[1] and for liquids and solutions of smaller molecules at low tempeatures.[2,3] As the effect depends on anisotropy of polarizability, the function studied is an average of second-rank spherical harmonics such as $P_2(\cos\theta(t)) = {}^1/_2(3\cos^2\theta(t) - 1)$, where $\theta(t)$ is the time-dependent angle between a molecular axis and the applied electric field. Because of this, Kerr-effect measurements are a valuable complement to studies of dielectric relaxation, in which the average is of permanent dipole orientation functions with symmetry $P_1(\cos\theta(t) = \cos\theta(t)$. For example, one can distinguish between diffusion-like and "large-jump" processes, as Williams and co-workers have shown.[2] A second kind of usefulness of the Kerr effect is in distinguishing between permanent dipole orientations and induced ionic charge displacements as polarization processes in biopolymers, as in studies by O'Konski and co-workers.[2]

A continuing difficulty in theoretical treatment of Kerr-effect relaxation, particularly for molecules with permanent dipole moments, arises from its nonlinearity with respect to applied field $E(t)$. The effect is necessarily an even function of $E(t)$, and even the limiting $E^2(t)$ behavior most easily observed presents problems. Most of the progress made has been for rotational diffusion models, and the simplest results of this kind from the classic work of Benoit[4,5] suffice to illustrate both the kinds of usefulness of Kerr-effect studies and the need for more general treatments.

Benoit considered axially symmetric molecules with permanent dipole moments μ along the axis of symmetry and an anisotropy $\Delta\alpha = \alpha_p - \alpha_s$ of polarizabilities α_p parallel and α_s perpendicular to this axis. Neglecting intermolecular correlation effects, the theoretical quantity derivable from Kerr experiments is the average, $\langle\Delta\alpha P_2(\cos\theta(t))f_E(t)\rangle$, where $f_E(t)$ is the time-dependent orientational distribution function for field $(E(t)$. Benoit obtained $f_E(t)$ by perturbation solution of the classical equation for forced

(1) For reviews, see articles in: "Molecular Electro-Optics, Electro-Optic Properties of Macromolecules and Colloids in Solution"; Krause, S., Ed.; Plenum Press: New York, 1981. See also artices in: "Molecular Electro-Optics"; O'Konoki, C. T., Ed.; Dekker: New York, 1976; Vol. 1, Parts 1 and 2.

(2) Beevers, M. S.; Crossley, J.; Garrington, D. C.; Williams, G. *J. Chem. Soc., Faraday Symp.* **1977**, *11*, 98.

(3) Beevers, M. S.; Elliott, D. A.; Williams, G. *J. Chem. Soc., Faraday Trans. 2* **1980**, *76*, 112.

(4) Benoit, H. *Ann. Phys. (Paris)* **1951**, *6*, 561.

(5) Benoit, H. *J. Chim. Phys. Phys.-Chim. Biol.* **1952**, *49*, 517.

0022-3654/82/2086-4700$01.25/0